Article

Driving Factors and Numerical Simulation of Evapotranspiration of a Typical Cabbage Agroecosystem in the Shiyang River Basin, Northwest China

Tianyi Yang [1,2,†], **Haichao Yu** [1,2,†], **Sien Li** [1,2,*], **Xiangning Yuan** [1,2], **Xiang Ao** [1,2], **Haochong Chen** [1,2], **Yuexin Wang** [1,2] **and Jie Ding** [1,2]

1 Center for Agricultural Water Research in China, China Agricultural University, Beijing 100083, China
2 National Field Scientific Observation and Research Station on Efficient Water Use of Oasis Agriculture in Wuwei of Gansu Province, Wuwei 733009, China
* Correspondence: lisien@cau.edu.cn
† These authors contributed equally to this work.

Abstract: Two years of field experiments were conducted at the National Field Observation Experiment Station for Efficient Agricultural Water Use in the Wuwei Oasis, Gansu Province. Based on the eddy correlation system, the evapotranspiration (*ET*) of the cabbage agroecosystem during the growth period was obtained and the main driving factors of *ET* changes were determined. The Root Zone Water Quality Model 2.0 version (RZWQM2 model) was used to simulate *ET* during the growth period. The results showed the following: (1) The *ET* of cabbage during the growth period was 260. 1 ± 24.2 mm, which was basically lower than other crops planted in this area. (2) Through partial correlation analysis and principal component analysis, it can be found that environmental and physiological factors jointly drive changes in *ET*. The main driving factors include gross primary productivity, net radiation, and water use efficiency. (3) The RZWQM2 model can simulate the *ET* of the cabbage agroecosystem well, especially in simulating the total *ET* value and its trend. The growth period ET_s were 7.3% lower than the ET_m. Cabbage is an important cash crop in Northwest China, and *ET* is an important component of the water cycle in the agroecosystem. Determining the main driving factors of *ET* is of great significance for the sustainable utilization of agricultural water resources in Northwest China. Our results can provide a scientific basis for the cultivation of cabbage as a cash crop and the development of water saving agriculture.

Keywords: evapotranspiration; agroecosystem; cabbages; eddy correlation system; driving factor

1. Introduction

Evapotranspiration (*ET*) is the main consumer of agricultural water, so it will be worthwhile to clarify its change pattern and driving factors during the growth period [1]. Previous studies have typically included environmental and physiological factors as variable indicators for studying the driving factors of *ET* [2–4]; however, for each agroecosystem, the main driving factors of *ET* are not the same. Zhou [5] pointed out, based on structural equation modeling, the radiation was the main driver of *ET* changes in the rainfed maize agroecosystem. Li [6] obtained similar results as Zhou [5] and concluded that a significant response was found between the leaf area and *ET*. Zhang [7] identified radiation, temperature, vapor pressure deficit, and wind speed as the main drivers. In summary, both environmental and physiological factors, such as leaf area, affect the change of *ET* during the growth period. However, most of the studies have focused on grain crops such as wheat and maize. In addition, most analyses of water fluxes have investigated the effects of environmental and physiological factors on changes in water use efficiency [8–10].

At present, there are two main ways to obtain *ET* on the field agroecosystem scale. One is direct observation, such as based on the eddy correlation system (EC system), large

aperture scintillometer [11], or a large weighing lysimeter [12]. To be more precise, the EC system can observe the changes in water fluxes at the field agroecosystem scale more continuously and accurately, and the application of this technology [13–15] effectively promotes the study of *ET* in fields. The other method is to simulate the *ET* during the growth period of crops through physical models and crop models. For instance, the Root Zone Water Quality Model Version 2.0 (RZWQM2 model) is a typical one that can accurately simulate the crop growth pattern and external environmental factors under different conditions. The RZWQM2 model couples the RZWQM model and the DSSAT model [16,17]. It has been proved by previous studies [18,19] to be able to accurately simulate plant height, leaf area, yield, *ET*, soil water content, and other factors during the growth period [20]. Saseendran [21] found that the *ET* of silage maize simulated by the RZWQM2 model was close to the accuracy of the observed data from a large weighing lysimeter. Zhang [22] simulated the *ET* of urban turf with different irrigation schedules based on the RZWQM2 model and developed a more reasonable irrigation schedule for urban turf in the North China Plain. Anapalli [23] simulated the *ET* of maize, soybean, and cotton agroecosystems in a humid climate based on the RZWQM2 model and found that the simulation accuracy was better at weekly scales than an EC system. In conclusion, the RZWQM2 model has been widely used to simulate the *ET* of crops with a clear mechanism and higher accuracy. As a cash crop widely planted in the arid region of Northwest China [1], cabbage has high yield and economic benefits. However, based on the literature research, there is little research on the driving factors of *ET* changes in cabbage agroecosystems in this area. We integrate the knowledge and methods of meteorology, agronomy, ecology, and other disciplines to fill the gap in the research on the driving factors of *ET* of typical cash crops in the arid region of Northwest China.

Understanding the changing patterns and drivers of *ET* is important for predicting the water use of agroecosystems under changing environments and ensuring sustainable use of water resources in SYRB [24,25]. SYRB is located in the east of the Hexi Corridor, at the intersection of the Qinghai Tibet Plateau, the Inner Mongolian Plateau and the Loess Plateau, and is an important sub basin of Yellow River. SYRB is an important agricultural production base and economic center in Gansu Province, China. It is an important ecological barrier and water source conservation area in Northwest China, and also a representative location for studying agricultural water resources in arid regions of China [26,27]. This area also grows cash crops such as tomatoes, potatoes, and cabbages [28]; however, water resources there are relatively scarce, while agroecosystems consumes the largest proportion of water in the basin [29]. As a result, water shortage is an important problem that restricts development of agriculture there. Hence, the study of water-saving agriculture will be significant for sustainable development of agriculture in the basin and the guaranteeing of water security in the area. Simulation of *ET* in a typical cabbage field by the RZWQM2 model helps to improve applicability of the model on the basis of clarifying the changing rules of *ET* during the growth period of the crop. In this study, three consecutive growth rotations were observed from 2020 to 2021 based on a typical cabbage agroecosystem in SYRB. This study has been conducted for the following reasons: (1) To investigate the changing patterns of *ET* and environmental factors during the growth period of cabbages. (2) To quantify the environmental and physiological factors that drive the changes in *ET* during the reproductive period of cabbages. (3) To use the experimental data to calibrate the RZWQM2 model in order to make it effectively simulate *ET* from typical cabbage agroecosystems in SYRB.

2. Materials and Methods

2.1. Study Area

During the growth period of cabbages in 2020 and 2021, a continuous observation experiment for three rotations was carried out at the Shiyanghe Experimental Station of China Agricultural University, Wuwei, Gansu Province, China (37°52′ N, 102°50′ E, 1581 m a.s.l.). The region has a typical temperate continental climate, with a multi-year average

precipitation of about 164.4 mm, which is mostly concentrated in July−September. The annual cumulative temperature (>0 °C) is about 3550 °C, the average annual sunshine duration is about 3000 h, the average annual pan evaporation is about 2000 mm [30], and the average depth of groundwater is about 25 m. The area has a high elevation, satisfying light and heat resources, and sufficient irrigation, which is suitable for growing cabbages and other vegetable crops [31]. The locations of the experimental station, observation instruments, and the cabbage field are shown in Figure 1.
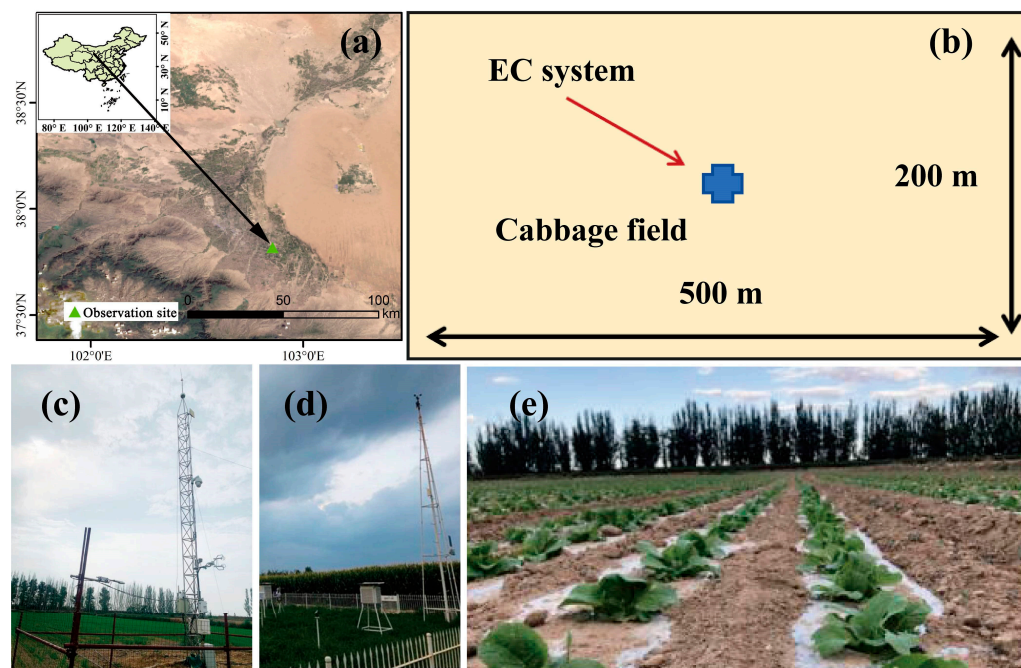

Figure 1. Overview the study area and field measurement. (**a**) Location of the experimental station. (**b**) Range of the observation plot. (**c**) The eddy covariance (EC) system. (**d**) The automatic weather station. (**e**) Cabbage field in the experimental station.

Cabbages were planted on a plot that was 500 m long and 250 m wide. Two rotations of cabbages were observed in 2020, with the start and end dates ranging from 2 May to 1 July and 1 August to 16 October in 2020, respectively, and from 9 April 2021 to 15 June in 2021, respectively. Cabbages were planted at a density of about 109,000 plants ha^{-1} at a sowing row spacing of 40 cm and a plant spacing of 23.0 cm. The specific dates and amounts of fertilizers applied are shown in Table 1.

Table 1. Types and application amounts of fertilizers for cabbages.

	Date	Type of Fertilization	Fertilizing Amount (kg hm^{-2})
20T1	2020/5/3	Urea (46% N)	150
	2020/5/11	Compound fertilizer (15% N–15% P$_2$O$_5$–15% K$_2$O)	188
	2020/5/19	Compound fertilizer (15% N–15% P$_2$O$_5$–15% K$_2$O)	188
	2020/5/29	Compound fertilizer (15% N–15% P$_2$O$_5$–15% K$_2$O)	188
	2020/6/3	Compound fertilizer (15% N–15% P$_2$O$_5$–15% K$_2$O)	188
	2020/6/13	Compound fertilizer (15% N–15% P$_2$O$_5$–15% K$_2$O)	188
20T2	2020/8/1	Urea (46% N)	150
	2020/8/12	Compound fertilizer (15% N–15% P$_2$O$_5$–15% K$_2$O)	188
	2020/8/18	Compound fertilizer (15% N–15% P$_2$O$_5$–15% K$_2$O)	188
	2020/8/27	Compound fertilizer (15% N–15% P$_2$O$_5$–15% K$_2$O)	188
	2020/9/5	Compound fertilizer (15% N–15% P$_2$O$_5$–15% K$_2$O)	188

Table 1. *Cont.*

	Date	Type of Fertilization	Fertilizing Amount (kg hm^{-2})
	2021/5/5	Urea (46% N)	150
21T3	2021/5/13	Compound fertilizer (15% N–15% P$_2$O$_5$–15% K$_2$O)	188
	2021/5/22	Compound fertilizer (15% N–15% P$_2$O$_5$–15% K$_2$O)	188
	2021/5/29	Compound fertilizer (15% N–15% P$_2$O$_5$–15% K$_2$O)	188

2.2. Eddy Correlation System

The study was based on the observation of water flux and the acquisition of radiation in a cabbage agroecosystem using an eddy covariance system (EC system) installed at a height of 2.5 m above the ground. The EC system mainly consists of temperature and humidity sensors (HMP45C, Vaisala, Vantaa, Finland), a Krypton hygrometer (KH20, Campbell Scientific, Inc., Logan, UT, USA), and a three-dimensional sonic anemometer/thermometer (CSAT3, Campbell Scientific, Inc., USA). Soil moisture was obtained using soil moisture sensors (CS616, Campbell Scientific Inc., USA) installed at different depths underground [32]. Based on the EC system, data of sensible heat flux and latent heat flux can be obtained and calculated with formulas as follows:

$$\lambda ET = \rho_a \overline{w'q'} \tag{1}$$

$$H = C_p \rho_a \overline{w'\,T'} \tag{2}$$

where λET and H are the latent and sensible heat flux (W m^{-2}), $\overline{w'q'}$ is the covariance between fluctuations of vertical wind speed w' (m s^{-1}) and humidity q' (kg kg^{-1}), $\overline{w'\,T'}$ is the covariance between fluctuations of w' and sonic temperature T' (K), ρ_a is the air density (kg m^{-3}), C_p the specific heat of dry air at constant pressure (J kg^{-1} K^{-1}), λ the latent heat of water vaporization (J kg^{-1}), and ET is the crop evapotranspiration (kg m^{-2} s^{-1}) [31].

The raw data obtained from observations were processed using Eddypro software (version 4.0, LI-Cor, Lincoln, NE, USA) to obtain water flux and latent heat flux. Subsequent data processing was conducted based on [33,34] to derive datasets used in this study. Missing data were interpolated using the method proposed by Guo [35]. The cabbage agroecosystem area is large enough and the field management measures are consistent enough to ensure the EC system obtains stable and continuous data. The vapor pressure deficit data used here were calculated based on the formula given in [36] using relative humidities and temperatures.

2.3. Plant Observation Indicators

During the experimental period, four cabbage plants with consistent growth conditions were selected every 7–10 days to observe their canopy height, leaf area [37], and biomass. The canopy height and leaf area were measured using a tape measure with an accuracy of 0.1 mm, and the formula for estimating leaf area was referenced in reference [38]:

$$LA = a \times \sum_{i=1}^{n} L_i \times W_i \tag{3}$$

where, LA is the leaf area (dm^2), a an empirical constant, L_i the length of the i-th leaf, W_i the width of the i-th leaf, and n is the number of leaves.

The measurement of biomass included both aboveground and belowground parts. Four cabbage plants were first placed in a 105 °C drying oven for 30 min for blanching. After that, the oven temperature was adjusted to 85 °C until constant weight was achieved. A balance with an accuracy of 0.01 g was used to weigh and sum the aboveground and belowground biomass to obtain the total biomass. For yield estimation, we selected 10 plots with an area of 2 m^2, weighed the aboveground parts during harvest, and calculated their average to estimate the crop yield.

2.4. Calculation of Water Use Efficiency

In this study, the water use efficiency (*WUE*) can be calculated as follows:

$$WUE = \frac{GPP}{ET} \tag{4}$$

where *WUE* is the agroecosystem water use efficiency (g C kg^{-1} H$_2$O) [39], *GPP* is gross primary productivity (g C m^{-2}), and the method of obtaining *GPP* can be found in [40].

2.5. Statistical Analysis

This study adopted partial correlation analysis and principal component analysis to determine the relationship between *ET* and its main driving factors during the experimental period. Partial correlation analysis can eliminate the influence from other factors on *ET*, with the formulae being as follows [41]:

$$R_{(X,Y)} = \frac{\sum_{i=1}^{n} \left(X_i - \overline{X}\right)\left(Y_i - \overline{Y}\right)}{\sqrt{\sum_{i=1}^{n}\left(X_i - \overline{X}\right)^2}\sqrt{\sum_{i=1}^{n}\left(Y_i - \overline{Y}\right)^2}} \tag{5}$$

$$R_{(i,j|h)} = \frac{R_{ij} - R_{ih}R_{jh}}{\sqrt{\left(1 - R_{ih}^2\right)\left(1 - R_{jh}^2\right)}} \tag{6}$$

where, $R_{(X,Y)}$ is the correlation between *X* and *Y* variables, X_i and Y_i are the values of the *i*-th *X* and *i*-th *Y* respectively, and $\overline{X}$ and $\overline{Y}$ are the average value of *X* and *Y*. $R_{(i,j|h)}$ is the partial correlation coefficient between variable *i* and *j* after excluding other variables, R_{ij} is the correlation coefficient between variable *i* and *j*, R_{ih} the correlation coefficient between variable *i* and *h*, and R_{jh} is the correlation coefficient between variable *j* and *h*.

Principal component analysis (PCA) has significant advantages in multidimensional data analysis and processing [42]. This method recombines interrelated multidimensional indicators into independent parts and analyzes them one by one to provide a reliable understanding of changes in *ET*. It can be found in reference [43]. Partial correlation analysis was performed using SPSS 25.0 (SPSS Inc., Chicago, IL, USA), while principal component analysis was performed using OriginPro 2021 (OriginLab., Northhampton, MA, USA) plotting and analysis software.

2.6. RZWQM2 Model

The RZWQM2 model can simulate daily scale crop *ET* [44]. Before *ET* simulation with this model, it is necessary to establish meteorological, soil, and field management data files. In this study, the data from the growth periods of cabbages in 2020 and 2021 were input into the RZWQM2 model, with the parameters being calibrated using the trial and error method. The physical parameters of soil at different soil depths are shown in Table 2:

Table 2. Physical parameters of soil at different depths.

Soil Depth (cm)	Soil Texture (%)				Bulk Density (g cm^{-3})	Saturated Hydraulic Conductivity (cm h^{-1})	Field Capacity Water Content (cm^3 cm^{-3})	Available Water Capacity (cm^3 cm^{-3})
		Sand	Silt	Clay				
0–20	silty loam	30.81	58.67	10.52	1.65	0.88	0.30	0.191
20–40	silty loam	19.43	68.25	12.32	1.69	0.64	0.29	0.185
40–60	silty loam	13.22	70.58	16.20	1.29	1.30	0.29	0.183
60–80	silty loam	10.38	74.87	14.75	1.48	0.75	0.32	0.209
80–100	silty loam	11.81	76.53	11.66	1.45	0.63	0.32	0.207

The accuracy of *ET* simulated by the RZWQM2 model is evaluated by the determination coefficient (R^2) and root mean square error (*RMSE*) using the following formulae:

$$RMSE = \sqrt{\frac{1}{n}\sum_{i=1}^{n}(P_i - O_i)^2} \tag{7}$$

$$R^2 = \left[\frac{\sum_{i=1}^{n}(O_i - O_{avg})(P_i - P_{avg})}{\sqrt{\sum_{i=1}^{n}(O_i - O_{avg})^2}\sqrt{\sum_{i=1}^{n}(P_i - P_{avg})^2}}\right]^2 \tag{8}$$

where, P_i is the *i*-th simulated value, and O_i is the *i*-th observed value; O_{avg} and P_{avg} are the average of simulated and observed values; *n* is the number of observed or simulated values.

3. Results

3.1. Dynamics of Environmental and Physiological Factors

Figure 2 shows the dynamics in environmental factors during the growth period of cabbages in 2020 and 2021. The daily average temperature (*Ta*) of the three rotations were 18.6 °C, 16.5 °C, and 16.2 °C. *Ta* dynamics during the first and third rotations (Figure 2(a1–a3)) were similar and showed a fluctuating downward trend during the second rotation (Figure 2(a2)). The daily average wind speed was 1.9 m s^{-1}, 1.1 m s^{-1} and 1.3 m s^{-1}, and the daily average relative humidity was 41.8%, 58.9% and 43.1%, respectively. The highest daily average relative humidity, approaching 60%, occurred in the second rotation (Figure 2(c2)). The total precipitation was 35.0 mm, 86.7 mm, and 52.8 mm, and the total irrigation amount was 160.4 mm, 133.5 mm, and 117.0 mm, respectively. The total irrigation amount was greater than the total precipitation.
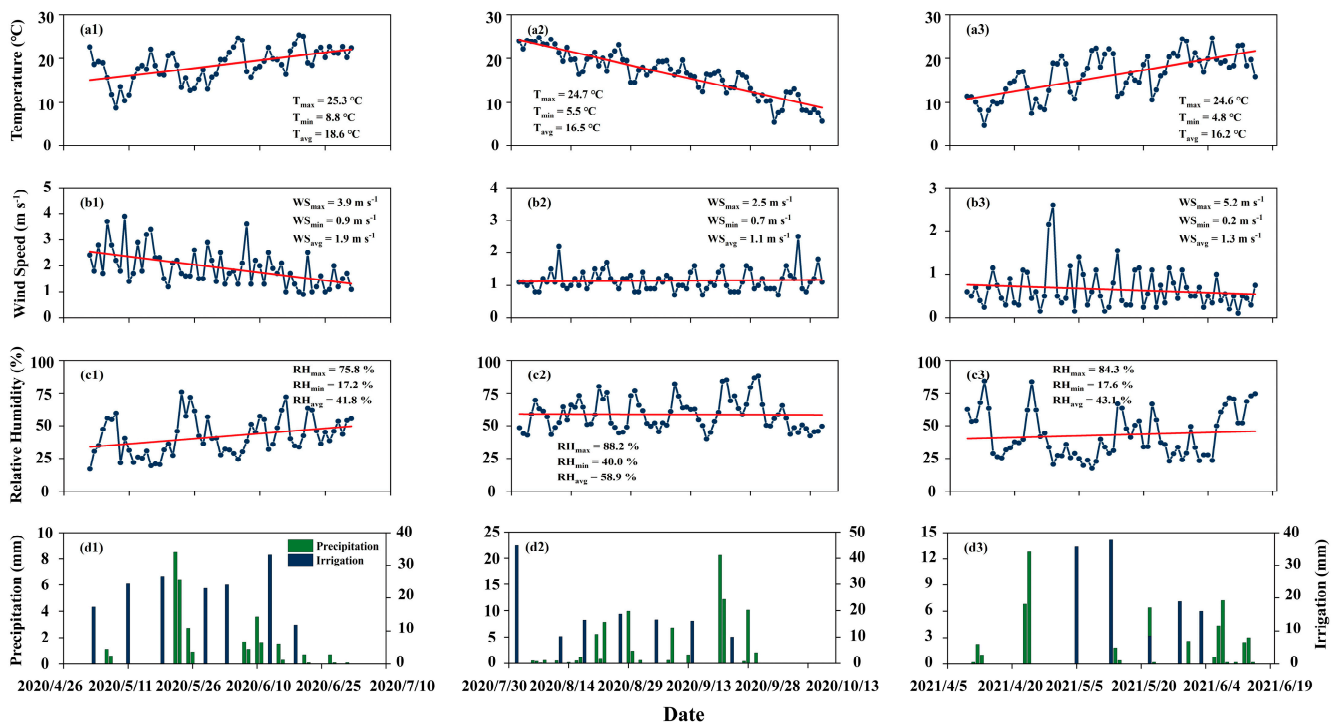

Figure 2. Daily average temperature (**a1–a3**); wind speed (**b1–b3**); relative humidity (**c1–c3**); irrigation and precipitation (**d1–d3**) during the growth period of cabbages.

Figure 3 shows the dynamics in the leaf area (*LA*), canopy height, and biomass of cabbages during the experimental period from 2020 to 2021. The variation patterns of *LA* during the three rotations are similar, with the maximum value happening during the maturity period, being 52.9 dm^2, 53.2 dm^2, and 38.3 dm^2, respectively. The dynamics in canopy height and *LA* illustrated in Figure 3(a1–a3,b1–b3) showed a similar trend. The

average canopy height during the seeding period hit the lowest, at 13.3 cm, 17.7 cm, and 12.6 cm, and it reached the highest during the maturity period, being 34.8 cm, 49.1 cm, and 38.7 cm, respectively. Figure 3(c1–c3) show the variation pattern of biomass, indicating rapid accumulation of biomass during the heading period and the maturity period. The maximum total biomass was 778.0 g m^{-2}, 512.3 g m^{-2}, and 825.0 g m^{-2}, respectively. The aboveground biomass took up a major part while the belowground biomass had a very small proportion after the seeding period. The aboveground biomass accounted for more than 90% of the total during the maturity period, with an average of 93.4%.
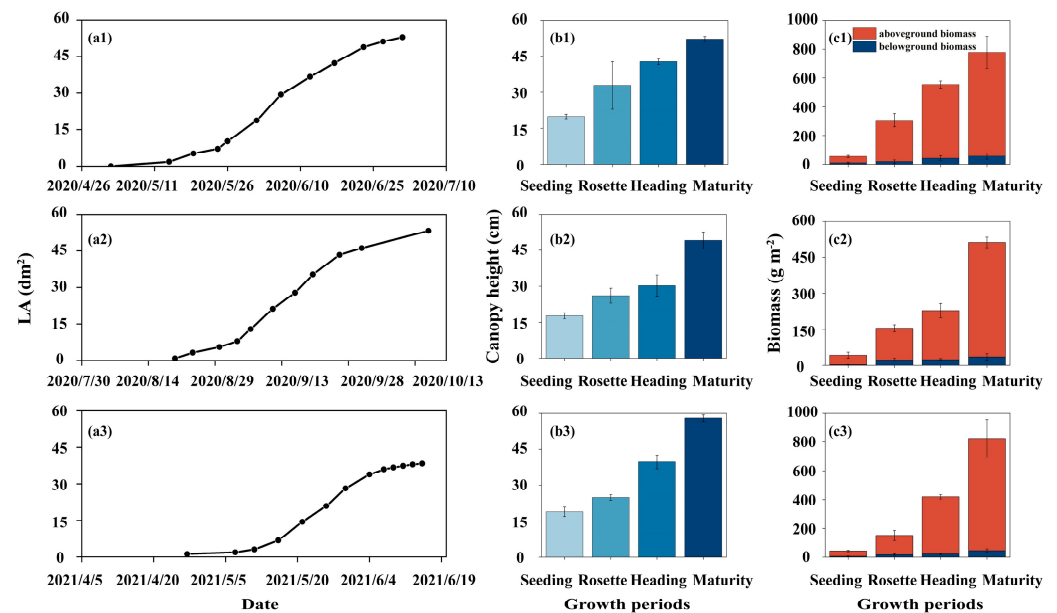

Figure 3. Dynamics of leaf area (LA) (**a1–a3**); canopy height (**b1–b3**); and biomass (**c1–c3**).

Figure 4 shows the variation patterns of *ET* and average water use efficiency (*WUE*) of cabbages in different growth periods during the experimental period. From Figure 4(a1–a3), it can be observed that, during the first rotation in 2020, the daily average *ET* during the seeding period, the rosette period, the heading period, and the maturity period was 1.8 mm d^{-1}, 4.5 mm d^{-1}, 6.6 mm d^{-1}, and 5.9 mm d^{-1}, respectively. The daily average *ET* values during the heading period and the maturity period were similar and at a high level, while the *ET* during the seeding period was significantly lower than that in other growth periods. During the second rotation, the *ET* increased first and then decreased, with the daily average *ET* during the seeding period, the rosette period, the heading period, and the maturity period being 2.8 mm d^{-1}, 4.4 mm d^{-1}, 4.5 mm d^{-1} and 2.4 mm d^{-1}, respectively. The daily average *ET* during the seeding period and the maturity period was relatively close. In contrast, during the third rotation, the daily average *ET* during the seeding period, the rosette period, the heading period, and the maturity period was 1.4 mm d^{-1}, 3.4 mm d^{-1}, 4.7 mm d^{-1}, and 6.2 mm d^{-1}, respectively, showing a fluctuating upward trend during four growth periods and reaching its highest in the maturity period. Similarly, during all three rotations, it was the smallest during the seeding period. In the experimental period, the precipitation was less than *ET*, which fully demonstrated the importance of irrigation for cabbage growth in SYRB.
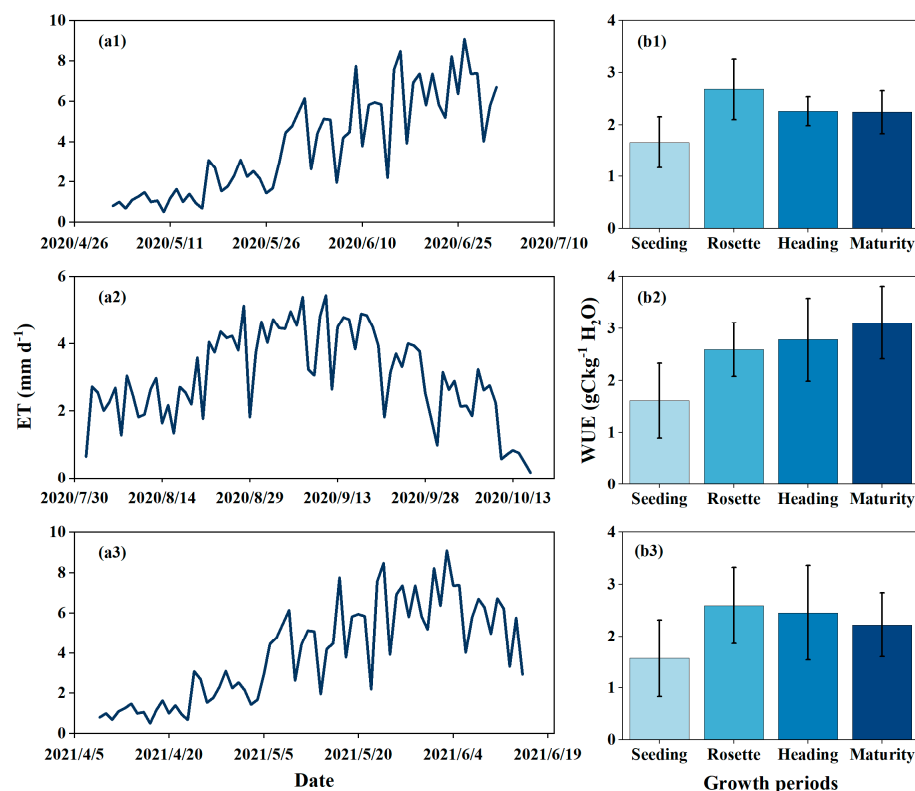
Figure 4. Dynamics of daily ET (**a1**–**a3**) and average WUE (**b1**–**b3**) in different growth periods.

The dynamics of the *WUE* of cabbages during the experimental period are shown in Figure 4(b1–b3). During the first rotation, the daily average *WUE* was the highest at 2.68 g C kg^{-1} H$_2$O in the rosette period. During the seeding period, the *WUE* reached the lowest at 1.66 g C kg^{-1} H$_2$O. The maximum *WUE* occurred on 29 May 2020, at 3.71 g C kg^{-1} H$_2$O. During the second rotation, the *WUE* of different growth periods showed a continuous increasing trend. The daily average *WUE* during the maturity period was 3.11 g C kg^{-1} H$_2$O, in contrast to 1.61 g C kg^{-1} H$_2$O during the seeding period. The highest daily *WUE* also occurred during the maturity period, at 4.89 g C kg^{-1} H$_2$O. The variation pattern of *WUE* during the third rotation was similar to that during the first rotation. The daily average *WUE* during the rosette period peaked at 2.59 g C kg^{-1} H$_2$O, while it hit the bottom during the seeding period, at 1.57 g C kg^{-1} H$_2$O. In summary, the daily average *WUE* hit its lowest point during the seeding period. The dynamics in the *WUE* of cabbages sown in the first half of the year were similar during different growth periods and were significantly different from those sown in the second half of the year.

3.2. The Drivers of ET

This study employed partial correlation analysis to investigate the driving factors of *ET* during the growth period of cabbages. Specifically, the environmental factors include net radiation (*Rn*), air temperature (*Ta*), soil moisture content at 20 cm depth (*SWC*), and vapor pressure deficit (*VPD*), and the physiological factors encompass the gross primary productivity (*GPP*), water use efficiency (*WUE*), and leaf area (*LA*). As shown in Figure 5, the *ET* of cabbages is mainly related to *GPP* (0.66), *Rn* (0.48), and *WUE* (−0.35). The importance of each factor to *ET* ranked in a descending order is as follows: *GPP* > *Rn* > *WUE* > *LA* > *SWC* > *VPD* > *Ta*. Among the main driving factors that cause changes in *ET*, *GPP* and *Rn* are positively correlated with *ET*, while *WUE* is negatively correlated with *ET*.
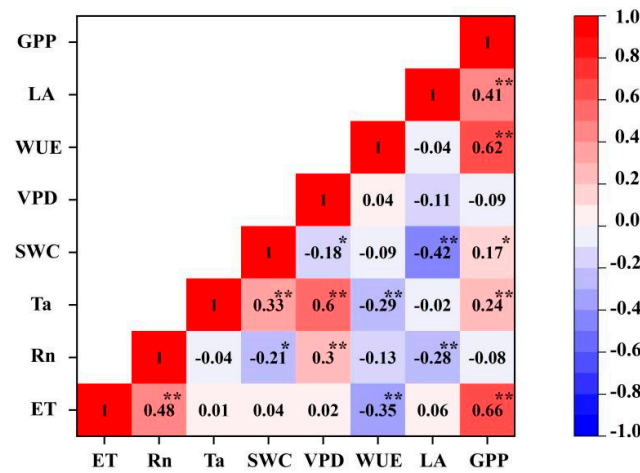
Figure 5. Correlation between ET and its main driving factors. * Indicating statistical significance ($p < 0.05$), ** Indicating statistical significance ($p < 0.01$).

Based on principal component analysis (PCA), the relationship between the *ET* of cabbages and its main driving factors was analyzed (Figure 6). The above factors were transformed into two orthogonal components, namely PC1 and PC2, which explained 69.8% of the total characteristic variance of *ET*. To be specific, PC1 could explain 43.0% of the total variance, with large loadings for *GPP*, *Rn* and *Ta*, while PC2 could explain 26.8%, with large loadings for *WUE* and *LA*. Among them, *GPP* and *Rn* are highly positively correlated with *ET*, while *WUE* is negatively correlated with *ET*. The results from principal component analysis are similar to those from partial correlation analysis.
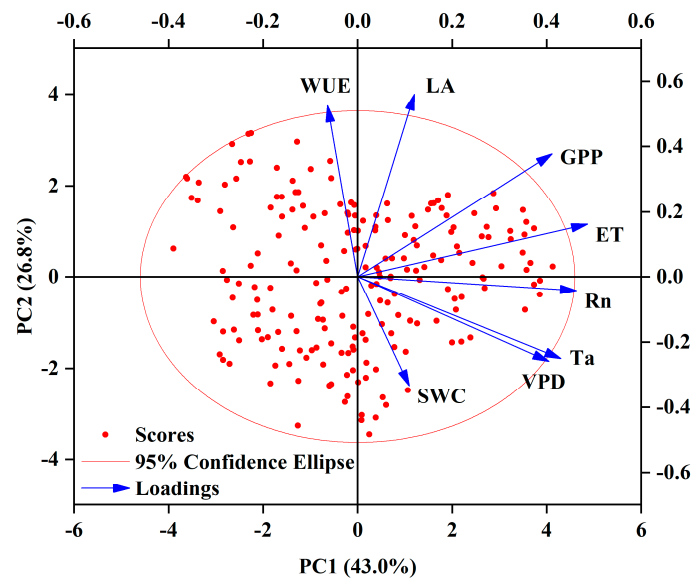

Figure 6. The biplot of principal components analysis (PCA) between *ET* and its drivers for the cabbages.

3.3. Simulation of ET with RZWQM2 Model

The RZWQM2 model has a good effect in regard to simulating the daily *ET* of cabbages. The measured evapotranspiration (ET_m) and simulated evapotranspiration (ET_s) values during the three rotations have the same trend. The ET_m during the whole growth period was 275.6 mm, 232.2 mm, and 272.5 mm, respectively. Based on the model simulation, the ET_s values were 256.9 mm, 215.1 mm, and 251.6 mm, respectively, 6.8%, 7.4%, and 7.7% lower than those of the ET_m, respectively, with the simulation accuracy being close to the research results of Kuang [45] and Hong [46]. Figure 7 shows the scatter plot of

all ET_m and ET_s data, with an R^2 of 0.73. The fitting relationship between the two is $ET_s = 0.77\,ET_m + 0.61$.
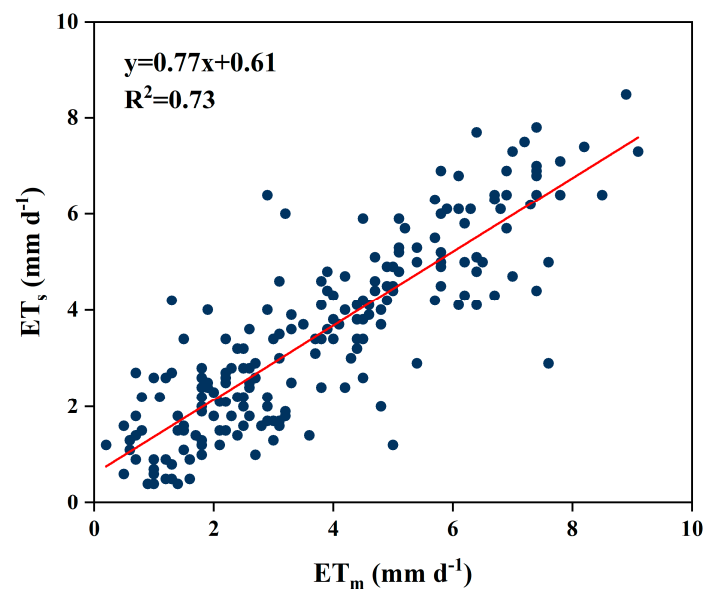

Figure 7. Scatter plot of ET_m and ET_s.

4. Discussions

4.1. ET, Yield and Economic Benefits

In order to understand the difference in ET between cabbages during the growth period and other similar studies in other regions, we collected the estimated ET for cabbages from previous studies (Table 3). As shown in the table, the ET of cabbages during the growth period varied from 141.4 mm to 296.3 mm in different studies. In this study, the total ET of cabbages during the growth period was 260.1 ± 24.2 mm. Based on the literature research, it can be found that there is a lack of research on the driving factors of ET in cabbage agricultural ecosystems in Northwest China. By comparing the ET during the growth period of other agricultural ecosystems in the arid region of Northwest China, it can be found that the ET of cabbage during the growth period is lower than that of other crops such as maize [47], wheat [48], and cotton [49].

During the experimental period, the average yield of cabbages was 8374.7 kg ha^{-1}, with an economic benefit of CNY 70,046.7 ha^{-1}. From an economic perspective, the comprehensive economic benefits of cabbages are better than other crops, such as maize [50], wheat [51], and soybean [52], which are mainly grown in this region. Considering the current situation of drought and low rainfall in this area, planting only one rotation of cabbages per year can reduce irrigation and increase economic benefits compared to planting other crops, thereby achieving the goal of water conservation and increasing income. It is worth noting that, unlike the grain crops, the price of cabbage fluctuates greatly and the initial investment is high, which may limit the large-scale cultivation of cabbage in Northwest China.

Table 3. Comparison of *ET* for different cabbage studies. Values of total *ET* during the growth period (total ET ± standard deviation).

Lat	Lon	Site	Type of the Crops	Irrigation Method	Length of Growth Period	ET (mm)	Ref.
41°21′ N	114°68′ E	Zhangjiakou, China	Chinese cabbage	Drip irrigation	59	214.8	(Zhou et al., 2020) [53]

Table 3. *Cont.*

Lat	Lon	Site	Type of the Crops	Irrigation Method	Length of Growth Period	ET (mm)	Ref.
22°57′ N	88°35′ E	West Bengal, India	Winter cabbage	Surface irrigation	90	223.2 ± 6.5	(Biswas et al., 2022) [54]
22°57′ N	88°35′ E	West Bengal, India	Winter cabbage	Surface irrigation	90	210.5 ± 6.5	(Biswas et al., 2022) [54]
28°38′ N	77°10′ E	New Delhi, India	Red cabbage	Drip irrigation	80	141.4 ± 19.9	(Kishor et al., 2024) [55]
38°04′ N	112°89′ E	Yangqu, Shanxi, China	Cabbage	Rainfed	98	296.3 ± 45.2	(Wang et al., 2024) [56]
37°52′ N	102°50′ E	Wuwei City	Cabbage	Drip irrigation	61	275.6	This study
37°52′ N	102°50′ E	Wuwei City	Cabbage	Drip irrigation	77	232.2	This study
37°52′ N	102°50′ E	Wuwei City	Cabbage	Drip Irrigation	68	272.5	This study

4.2. The Drivers of ET

Studying the driving factors of *ET* is of great significance in understanding the change mechanism of agroecosystem *ET* and formulating agricultural water saving policies. Previous studies on the driving factors of agroecosystem *ET* are relatively limited, with a focus on the driving factors of *WUE*. Fang [57] showed that the *ET* of maize during its growth period is mainly influenced by meteorological factors, while, in this study, only temperature, wind speed and net radiation were considered. Li [58] pointed out that net radiation, *VPD*, and temperature are the three main driving factors leading to changes in *ET*, but this study lacks consideration of physiological factors. Chu [59] considered that net radiation dominates the changes in crop *ET* during the summer growth period in the Huai River Basin, while wind speed dominates the changes in *ET* during non-summer and plant growth seasons. Zhao [60] evaluated the contributions of environmental and physiological factors on the agroecosystem scale to soil evaporation and vegetation transpiration based on observations of EC systems, believing that *VPD* is the main factor driving soil evaporation changes while available energy above the canopy is the main factor driving vegetation transpiration changes. In summary, in existing studies on driving factors of agroecosystem *ET*, most studies have included a relatively small number of driving factors. The agroecosystem-scale studies mostly focus on grain crops such as wheat and maize while paying little attention to the driving factors of changes in cabbage *ET*. This study considered physiological factors including *WUE*, *GPP*, and *LAI*, as well as environmental factors such as *Rn*, *Ta*, *SWC*, and *VPD*. Compared with previous studies, this study has considered the effects of multiple factors on *ET* changes. The results show that *GPP* is the main driving factor for *ET* changes during the growth period of cabbages.

4.3. Uncertainty and Significance of the Research

We analyzed the driving factors for changes in the *ET* of cabbages based on 2-year experimental data and comprehensively considered the combined effects of environmental and physiological factors. In addition to the factors considered here, *ET* may also be influenced by CO_2 concentration [61]. The change in CO_2 concentration leads to changes in carbon flux and, in turn, affects *ET* [62]. In addition to CO_2 concentration, field management measures and soil fertility may also have an impact on *ET*. In the future, more factors driving the change in *ET* may be included in the research. Clarifying the variation patterns and influencing factors of *ET* is of great significance for understanding the value of *ET* in the changing environment and clarifying the mechanism of interaction between the environment and crops.

5. Conclusions

Based on our research, the following conclusions can be drawn: (1) During the growth period of cabbages from 2020 to 2021, the *ET* of cabbages was 260.1 ± 24.2 mm, which was basically lower than that of other crops in SYRB. (2) Through partial correlation analysis and principal component analysis, it can be found that environmental and physiological factors jointly drive the changes in *ET* during the growth period of cabbages in SYRB. Among them, *GPP*, *Rn* and *WUE* are the main factors driving the changes in *ET*. (3) The RZWQM2 model can simulate the *ET* of a cabbage agroecosystem in the SYRB and has a good result in simulating the total *ET* value and the trend of *ET* changes. The growth period scale ET_s are 7.3% lower than the ET_m.

Based on the EC system, this study observed the ET during the growth period of a typical cabbage agroecosystem in the SYRB, analyzing the main driving factors that led to the change in ET and simulated the change in ET through the RZWQM2 model. Our research observation period is two years, and we can conduct longer observations of the cabbage agroecosystem. This study is of great significance for adjusting crop planting structures and efficiently utilizing agricultural water resources in Northwest China.

Author Contributions: T.Y.: writing—original draft preparation and writing—review and editing, H.Y.: writing—original draft preparation and writing—review and editing, S.L.: project administration and funding acquisition, X.Y.: methodology and software, X.A.: validation and investigation, H.C.: formal analysis and supervision, Y.W.: resources and conceptualization, J.D. data curation. All authors have read and agreed to the published version of the manuscript.

Institutional Review Board Statement: Not applicable.

Data Availability Statement: Data are contained within the article.

Conflicts of Interest: The authors declare no conflict of interest.

References

1. Yu, H.; Li, S.; Ding, J.; Yang, T.; Wang, Y. Water use efficiency and its drivers of two typical cash crops in an arid area of Northwest China. *Agric. Water Manag.* **2023**, *287*, 108433. [CrossRef]
2. Gao, L.; Zhao, P.; Kang, S.; Li, S.; Tong, L.; Ding, R.; Lu, H. Surface soil water content dominates the difference between ecosystem and canopy water use efficiency in a sparse vineyard. *Agric. Water Manag.* **2019**, *226*, 105817. [CrossRef]
3. Wang, W.; Wang, X.; Huo, Z.; Rong, Y.; Huang, Q.; Huang, G. Variation and attribution of water use efficiency in sunflower and maize fields in an irrigated semi-arid area. *Hydrol. Process.* **2021**, *35*, e14080. [CrossRef]
4. Li, Y.; Fan, J.; Hu, Z.; Shao, Q.; Harris, W. Comparison of evapotranspiration components and water-use efficiency among different land use patterns of temperate steppe in the Northern China pastoral-farming ecotone. *Int. J. Biometeorol.* **2016**, *60*, 827–841. [CrossRef] [PubMed]
5. Zhou, L.; Wang, Y.; Jia, Q.; Li, R.; Zhou, M.; Zhou, G. Evapotranspiration over a rainfed maize field in northeast China: How are relationships between the environment and terrestrial evapotranspiration mediated by leaf area. *Agric. Water Manag.* **2019**, *221*, 538–546. [CrossRef]
6. Li, Y.; Shi, H.; Zhou, L.; Eamus, D.; Huete, A.; LI, L.; Cleverly, J.; Hu, Z.; Harahap, M.; Yu, Q.; et al. Disentangling Climate and LAI Effects on Seasonal Variability in Water Use Efficiency Across Terrestrial Ecosystems in China. *J. Geophys. Res. Biogeosci.* **2018**, *129*, 2429–2443. [CrossRef]
7. Zhang, B.; Xu, D.; Liu, Y.; Li, F.; Cai, J.; Du, L. Multi scale evapotranspiration of summer maize and the controlling meteorological factors in north China. *Agric. For. Meteorol.* **2016**, *216*, 1–12. [CrossRef]
8. Jiang, S.; Liang, C.; Cui, N.; Zhao, L.; Liu, C.; Feng, Y.; Hu, X.; Gong, D.; Zou, Q. Water use efficiency and its drivers in four typical agroecosystems based on flux tower measurements. *Agric. For. Meteorol.* **2020**, *295*, 108200. [CrossRef]
9. Wang, Y.; Zhou, L.; Ping, X.; Jia, Q.; Li, R. Ten-year variability and environmental controls of ecosystem water use efficiency in a rainfed maize cropland in Northeast China. *Field Crops Res.* **2018**, *226*, 48–55. [CrossRef]
10. Xie, J.; Zha, T.; Zhou, C.; Jia, X.; Yu, H.; Yang, B.; Chen, J.; Zhang, F.; Wang, B.; Bourque, C.; et al. Seasonal variation in ecosystem water use efficiency in an urban-forest reserve affected by periodic drought. *Agric. For. Meteorol.* **2016**, *221*, 142–151. [CrossRef]
11. Liu, S.; Xu, Z.; Zhu, Z.; Jia, Z.; Zhu, M. Measurements of evapotranspiration from eddy-covariance systems and large aperture scintillometers in the Hai River Basin, China. *J. Hydrol.* **2013**, *487*, 24–38. [CrossRef]

12. Liu, C.; Cui, N.; Gong, D.; Hu, X.; Yu, F. Evaluation of seasonal evapotranspiration of winter wheat in humid region of East China using large-weighted lysimeter and three models. *J. Hydrol.* **2020**, *590*, 125388. [CrossRef]

13. Zhang, Y.; Guo, X.; Pei, H.; Min, L.; Liu, F.; Shen, Y. Evapotranspiration and carbon exchange of the main agroecosystems and their responses to agricultural land use change in North China Plain. *Agric. Ecosyst. Environ.* **2022**, *338*, 108103. [CrossRef]

14. Wang, X.; Lei, H.; Li, J.; Qu, Y.; Kong, D.; Huo, Z. Climate and management impacts on the spatiotemporal dynamics of water-carbon fluxes in the North China Plain. *Agric. Ecosyst. Environ.* **2023**, *343*, 108270. [CrossRef]

15. Wang, Y.; Li, S.; Cui, Y.; Qin, S.; Guo, H.; Yang, D.; Wang, C. Effect of Drip Irrigation on Soil Water Balance and Water Use Efficiency of Maize in Northwest China. *Water* **2021**, *13*, 217. [CrossRef]

16. Saseendran, S.; Ahuja, L.; Ma, L.; Nielsen, D.; Andales, T.; Chávez, A.; Ham, J. Enhancing the Water Stress Factors for Simulation of Corn in RZWQM2. *Agronomy* **2014**, *106*, 81–94. [CrossRef]

17. Dokoohaki, H.; Gheysari, M.; Mousavi, S.; Zand-Parsa, S.; Miguez, F.; Archontoulis, S.; Hoogenboom, G. Coupling and testing a new soil water module in DSSAT CERES-Maize model for maize production under semi-arid condition. *Agric. Water Manag.* **2016**, *163*, 90–99. [CrossRef]

18. Ding, J.; Hu, W.; Wu, J.; Yang, Y.; Feng, H. Simulating the effects of conventional versus conservation tillage on soil water, nitrogen dynamics, and yield of winter wheat with RZWQM2. *Agric. Water Manag.* **2020**, *230*, 105956. [CrossRef]

19. Chen, X.; Qi, Z.; Gui, D.; Gu, Z.; Ma, L.; Zeng, F.; Li, L. Simulating impacts of climate change on cotton yield and water requirement using RZWQM2. *Agric. Water Manag.* **2019**, *222*, 231–241. [CrossRef]

20. Fang, Q.; Ma, L.; Yu, Q.; Ahuja, L.; Malone, R.; Hoogenboom, G. Irrigation strategies to improve the water use efficiency of wheat--maize double cropping systems in North China Plain. *Agric. Water Manag.* **2010**, *97*, 1165–1174. [CrossRef]

21. Anapalli, S.; Ahuja, L.; Gowda, P.; Ma, L.; Marek, G.; Evett, S.; Howell, T. Simulation of crop evapotranspiration and crop coefficients with data in weighing lysimeters. *Agric. Water Manag.* **2016**, *177*, 274–283. [CrossRef]

22. Zhang, H.; Wang, J.; Liu, M.; Shen, Y.; Pei, H. Water Budget of Urban Turf Field and Optimal Irrigation Schedule Simulation in an Ecotone between Semi-Humid and Semi-Arid Regions, Northern China. *Agronomy* **2023**, *13*, 273. [CrossRef]

23. Anapalli, S.; Fisher, D.; Reddy, K.; Rajan, N.; Pinnamaneni, S. Modeling evapotranspiration for irrigation water management in a humid climate. *Agric. Water Manag.* **2019**, *225*, 105731. [CrossRef]

24. Chen, Y.; Xue, Y.; Hu, Y. How multiple factors control evapotranspiration in North America evergreen needleleaf forests. *Sci. Total Environ.* **2018**, *622–623*, 1217–1224. [CrossRef] [PubMed]

25. Fisher, J.; Melton, F.; Middleton, E.; Hain, C.; Anderson, M.; Allen, R.; McCabe, M.; Hook, S.; Baldocchi, D.; Townsend, P.; et al. The future of evapotranspiration: Global requirements for ecosystem functioning, carbon and climate feedbacks, agricultural management, and water resources. *Water Resour. Res.* **2017**, *53*, 2618–2626. [CrossRef]

26. Yang, D.; Li, S.; Wu, M.; Yang, H.; Zhang, W.; Chen, J.; Wang, C.; Huang, S.; Zhang, R.; Zhang, Y. Drip irrigation improves spring wheat water productivity by reducing leaf area while increasing yield. *Eur. J. Agron.* **2023**, *143*, 126710. [CrossRef]

27. Wang, Y.; Li, S.; Qin, S. How can drip irrigation save water and reduce evapotranspiration compared to border irrigation in arid regions in northwest China. *Agric. Water Manag.* **2020**, *239*, 106256. [CrossRef]

28. Chen, J.; Kang, S.; Du, T.; Qiu, R.; Guo, P.; Chen, R. Quantitative response of greenhouse tomato yield and quality to water deficit at different growth stages. *Agric. Water Manag.* **2023**, *129*, 152–162. [CrossRef]

29. *2021 Annual Report on Water Resources in Gansu Province*; Gansu Water Resources Department: Lanzhou, China; Shanxi Publishing House: Taiyuan, China, 2020.

30. Li, S.; Zhang, L.; Kang, S.; Tong, L.; Du, T.; Hao, X.; Zhao, P. Comparison of several surface resistance models for estimating crop evapotranspiration over the entire growing season in arid regions. *Agric. For. Meteorol.* **2015**, *208*, 1–15. [CrossRef]

31. Ding, J.; Li, S.; Wang, H.; Wang, C.; Zhang, Y.; Yang, D. Estimation of Evapotranspiration and Crop Coefficient of Chinese Cabbage Using Eddy Covariance in Northwest China. *Water* **2021**, *13*, 2781. [CrossRef]

32. Qin, S.; Li, S.; Cheng, L.; Zhang, L.; Qiu, R.; Liu, P.; Xi, H. Partitioning evapotranspiration in partially mulched interplanted croplands. *Agric. Water Manag.* **2023**, *276*, 108040. [CrossRef]

33. Yu, G.R.; Sun, X.M. *Principles of Flux Measurement in Terrestrial Ecosystems*; Higher Education Press: Beijing, China, 2006.

34. Qin, S.; Li, S.; Kang, S.; Du, T.; Tong, L.; Ding, R.; Wang, Y.; Guo, H. Transpiration of female and male parents of seed maize in northwest China. *Agric. Water Manag.* **2019**, *213*, 397–409. [CrossRef]

35. Guo, H.; Li, S.; Kang, S.; Du, T.; Tong, L.; Hao, X.; Ding, R. Crop coefficient for spring maize under plastic mulch based on 12-year eddy covariance observation in the arid region of Northwest China. *J. Hydrol.* **2020**, *588*, 125108. [CrossRef]

36. Allen, R.G.; Pereira, L.S.; Raes, D.; Martin, S. *Crop Evapotranspiration Guidelines for Computing Crop Water Requirements*; FAO Irrigation and Drainage Paper No.56; FAO: Rome, Italy, 1998; pp. 147–148.

37. Qin, S.; Fan, Y.; Li, S.; Cheng, L.; Zhang, L.; Xi, H.; Qiu, R.; Liu, P. Partitioning of available energy in canopy and soil surface in croplands with different irrigation methods. *Agric. Water Manag.* **2023**, *288*, 108475. [CrossRef]

38. Guo, H.; Li, S.; Kang, S.; Du, T.; Tong, L.; Ding, R. Annual ecosystem respiration of maize was primarily driven by crop growth and soil water conditions. *Agric. Ecosyst. Environ.* **2019**, *272*, 254–265. [CrossRef]

39. Yu, G.; Song, X.; Wang, Q.; Liu, Y.; Guan, D.; Yan, J.; Sun, X.; Zhang, L.; Wen, X. Water-use efficiency of forest ecosystems in eastern China and its relations to climatic variables. *New Phytol.* **2008**, *177*, 927–937. [CrossRef]

40. Guo, H.; Li, S.; Kang, S.; Du, T.; Liu, W.; Tong, L.; Hao, X.; Ding, R. The controlling factors of ecosystem water use efficiency in maize fields under drip and border irrigation systems in Northwest China. *Agric. Water Manag.* **2022**, *272*, 107839. [CrossRef]

41. Chen, J.; Shao, Z.; Deng, X.; Huang, X.; Dang, C. Vegetation as the catalyst for water circulation on global terrestrial ecosystem. *Sci. Total Environ.* **2023**, *895*, 165071. [CrossRef] [PubMed]

42. Chang, L.; Liou, J.; Chang, F. Spatial-temporal flood inundation nowcasts by fusing machine learning methods and principal component analysis. *J. Hydrol.* **2022**, *612*, 128086. [CrossRef]

43. Zhao, X.; Zhang, H.; Li, T.; Ye, Z.; Xue, C.; Zhang, Y.; Yang, Z. Types identification and development tracking of urban water scarcity in China: A case study of 32 major cities. *J. Nat. Resour.* **2023**, *38*, 2619–2636. [CrossRef]

44. Gu, Z.; Qi, Z.; Ma, L.; Gui, D.; Xu, J.; Fang, Q.; Yuan, S.; Feng, G. Development of an irrigation scheduling software based on model predicted crop water stress. *Comput. Electron. Agric.* **2017**, *132*, 208–221. [CrossRef]

45. Kuang, N.; Ma, Y.; Hong, S.; Jiao, F.; Liu, C.; Li, Q.; Han, H. Simulation of soil moisture dynamics, evapotranspiration, and water drainage of summer maize in response to different depths of subsoiling with RZWQM2. *Agric. Water Manag.* **2021**, *249*, 106794. [CrossRef]

46. Hong, S.; Jiao, F.; Kuang, N.; Liu, C.; Ma, Y.; Li, Q. Simulating the effects of irrigation and tillage on soil water, evapotranspiration, and yield of winter wheat with RZWQM2. *Soil Tillage Res.* **2021**, *214*, 105170. [CrossRef]

47. Wang, C.; Li, S.; Wu, M.; Zhang, W.; He, H.; Yang, D.; Huang, S.; Guo, Z.; Xing, X. Water use efficiency control for a maize field under mulched drip irrigation. *Sci. Total Environ.* **2023**, *857*, 159457. [CrossRef] [PubMed]

48. Yang, D.; Li, S.; Kang, S.; Du, T.; Guo, P.; Mao, X.; Tong, L.; Mao, X.; Tong, L.; Hao, X.; et al. Effect of drip irrigation on wheat evapotranspiration, soil evaporation and transpiration in Northwest China. *Agric. Water Manag.* **2020**, *232*, 106001. [CrossRef]

49. Ge, R. Study of Evapotranspiration Law and Water Demand Model of Cotton Field in Drip Irrigation Oasis under Mulch. Master's Thesis, Shihezi University, Shihezi, China, 2020.

50. Wang, Y. Mechanism and Simulation of Water and Nitrogen Transport in the Maize Field under Different Irrigation Methods. Ph.D. Thesis, China Agricultural University, Beijing, China, 2021.

51. Li, J. Study on the Effects of Different Irrigation Methods on Water Heat Transfer and Growth of Spring Wheat. Master's Thesis, China Agricultural University, Beijing, China, 2018.

52. Liao, Z.; Pei, S.; Bai, Z.; Lai, Z.; Wen, L.; Zhang, F.; Li, Z.; Fan, J. Economic evaluation and risk premium estimation of rainfed soybean under various planting practices in a semi-humid drought-prone region of Northwest China. *Agronomy* **2023**, *13*, 2840. [CrossRef]

53. Zhou, L.; Ye, S.; Xu, F.; Li, Y.; Cen, J. Evapotranspiration characteristic and water saving potential of Chinese cabbage under mulched drip irrigation in cold regions. *J. Drain. Irrig. Mach. Eng.* **2020**, *38*, 194–199. (In Chinese)

54. Biswas, T.; Bandyopadhyay, P.; Nandi, R.; Mukherjee, S.; Kundu, A.; Reddy, P.; Mandal, B.; Kumar, P. Impact of mulching and nutrients on soil water balance and actual evapotranspiration of irrigated winter cabbage (*Brassica oleracea* var. capitata L.). *Agric. Water Manag.* **2022**, *263*, 107456.

55. Kishor, N.; Manoj, K.; Rajanna, G.; Man, S.; Anupama, S.; Shrawan, S.; Tirthankar, B.; Neeraj, P.; Jitendra, R.; Kiruthiga, B. Soil water distribution and water productivity in red cabbage crop using superabsorbent polymeric hydrogels under different drip irrigation regimes. *Agric. Water Manag.* **2024**, *295*, 108759.

56. Wang, X.; Wang, T.; Wang, L.; Liu, E. The Effects of Different Rotations of Beans, Maize, and Cabbage on Soil Moisture and Economic Benefits. *Agronomy* **2024**, *14*, 479. [CrossRef]

57. Fang, B.; Lei, H.; Zhang, Y.; Quan, Q.; Yang, D. Spatio-temporal patterns of evapotranspiration based on upscaling eddy covariance measurements in the dryland of the North China Plain. *Agric. For. Meteorol.* **2020**, *281*, 107844. [CrossRef]

58. Li, S.; Kang, S.; Zhang, L.; Zhang, J. On the attribution of changing crop evapotranspiration in arid regions using four methods. *J. Hydrol.* **2018**, *563*, 576–585. [CrossRef]

59. Chu, R.; Li, M.; Islam, A.; Fei, D.; Shen, S. Attribution analysis of actual and potential evapotranspiration changes based on the complementary relationship theory in the Huai River basin of eastern China. *Int. J. Climatol.* **2019**, *39*, 4072–4090. [CrossRef]

60. Zhao, P.; Kang, S.; Li, S.; Ding, R.; Tong, L.; Du, T. Seasonal variations in vineyard ET partitioning and dual crop coefficients correlate with canopy development and surface soil moisture. *Agric. Water Manag.* **2018**, *197*, 19–33. [CrossRef]

61. Keenan, T.; Hollinger, D.; Bohrer, G.; Dragoni, D.; Munger, W.; Schmid, H.; Richardson, A. Increase in forest water-use efficiency as atmospheric carbon dioxide concentrations rise. *Nature* **2013**, *499*, 324–328. [CrossRef] [PubMed]

62. Saurer, M.; Siegwolf, R.; Schweingruber, F. Carbon isotope discrimination indicates improving water-use efficiency of trees in northern Eurasia over the last 100 years. *Global Chang. Biol.* **2004**, *10*, 2109–2120. [CrossRef]